

PRODUCTION, MICROSTRUCTURE AND TRIBOLOGICAL PROPERTIES OF Zn-AI/Ti METAL-METAL COMPOSITES REINFORCED WITH ALUMINA NANOPARTICLES

Aleksandar Vencl 

University of Belgrade, Faculty of Mechanical Engineering, Kraljice Marije 16, 11120 Belgrade 35, Serbia
South Ural State University, Lenin prospekt 76, 454080 Chelyabinsk, Russia

Veljko Šljivić

University of Belgrade, Faculty of Mechanical Engineering, Kraljice Marije 16, 11120 Belgrade 35, Serbia

Marcela Pokusová

Faculty of Mechanical Engineering, Slovak University of Technology in Bratislava, Ná mestie Slobody 17, 812 31 Bratislava, Slovakia

Mara Kandeva

Faculty of Industrial Technology, Technical University of Sofia, 8 Kliment Ohridski Blvd, 1000 Sofia, Bulgaria
South Ural State University, Lenin prospekt 76, 454080 Chelyabinsk, Russia

HongGuang Sun

Institute of Hydraulics and Fluid Mechanics, College of Mechanics and Materials, Hohai University, Xikang Road 1, 210098 Nanjing, China

Elena Zadorozhnaya

South Ural State University, Lenin prospekt 76, 454080 Chelyabinsk, Russia

Ilija Bobić

Institute of Nuclear Sciences “Vinca”, University of Belgrade, Mike Petrovića Alasa 12-14, 11001 Belgrade, Serbia

Copyright © 2021 American Foundry Society
<https://doi.org/10.1007/s40962-020-00565-5>

Abstract

The investigated metal-metal composites were produced by the compocasting process using the standard zinc-aluminium alloy ZA-27 as a matrix and titanium microparticles (particle size approx. 10 μm) as a secondary phase. The amount of Ti microparticles was 1 and 2 wt%. Small amount (0.5 wt%) of alumina nanoparticles (particle size 20–30 nm) is also used, as reinforcement. The aim of the presented research was to evaluate the possibility of producing such composites, as well as to see the effect of the addition of Ti microparticles and/or alumina nanoparticles on their microstructure, mechanical and tribological properties. Microstructure and worn surfaces analysis were performed by scanning electron microscope, and mechanical properties were analysed through the Vickers microhardness values. Tribological properties were

determined on tribometer with line contact, under mixed lubrication conditions. Microstructural analysis showed that the distribution of Ti microparticles has been improved due to the addition of Al_2O_3 nanoparticles. This better distribution did not show any significant influence on the microhardness values or coefficient of friction values of the composites, but it induced higher wear resistance of metal-metal composites reinforced with Al_2O_3 nanoparticles. Better distribution and higher amount of Ti particles increased the surface area of the matrix that was protected with Ti particles during sliding and reduced wear.

Keywords: ZA-27 alloy, metal-metal composites, nanoparticles, microstructure, friction, wear

Introduction

The ZA-27 is well-known zinc and aluminium alloy and has the highest strength and the lowest density of all standardized alloys.¹ It is resistant to atmospheric corrosion and possesses good tribological properties, which enabled its use as a material for sliding bearings.^{2,3} Many efforts have been conducted to improve the mechanical properties of ZA alloys, the most important of which are heat treatment, mechanical processing, semi-solid processing and alloying.⁴ Although its tribological properties are very good, they can be improved further by adding hard ceramic microparticles to the alloy, i.e. by producing metal matrix composites (MMCs).⁵ Added reinforcement particles limit the dislocation mobility, thereby improving the strength properties.⁶ However, these added ceramic particles usually reduce the ductility of the matrix. The main reason for this decrease in ductility is differences between the metal matrix and ceramic reinforcement (different nature of internal bonds and large mismatch of the elastic modulus and coefficient of thermal expansion).⁷

Metal-metal composites are sometimes used to overcome the limitations of MMCs reinforced with ceramic (metal-ceramic composites). The metal-metal composites are combination of two metals or alloys with different physical and mechanical properties, which provide properties that cannot be obtained from individual phases. Pure titanium (in an oxygen-free environment) is a ductile metal and has relatively high strength and low density, i.e. high strength-to-weight ratio. Titanium melting point is much higher than the melting point of ZA-27 alloy, so the alloying is not possible. It is assumed that this has an effect on improving the mechanical properties of the produced metal-metal composite at elevated temperatures. Due to their low density, light metals are most frequently used matrix metals, but there are only a few researches which apply the titanium powder as a secondary phase in aluminium^{8,9} or magnesium^{10–12}-based metal-metal composites. These researches are relatively new, and there are no such investigations on composites with the Zn-Al alloy base. The presence of ceramic nanoparticles creates the fine-grained structure of the matrix alloy (ZA-27), which enhances the mechanical properties of the composite.¹³

The aim of the presented research was to evaluate the possibility of producing the metal-metal composites with Zn-Al alloy base and addition of Ti microparticles and alumina nanoparticles. The initial and basic structural, mechanical and tribological characterization was performed to indicate the direction and perspective of further work on the development of these metal-metal composites.

Experimental Details

Materials

Matrix was zinc-aluminium alloy ZA-27, with the chemical composition according to the ASTM standard,¹⁴ i.e. 25–28

Table 1. Designation of the Produced Metal-Metal Composites and Used Reinforcements

Metal-metal composite designation	Reinforcement amount, wt%	
	Ti microparticles (approx. 10 μm)	Al ₂ O ₃ nanoparticles (20–30 nm)
1Ti	1	–
1Ti-0.5Al ₂ O ₃	1	0.5
2Ti-0.5Al ₂ O ₃	2	0.5

wt% Al, 2–2.5 wt% Cu, 0.01–0.02 wt% Mg, and Zn as remainder. Type, size and amount of reinforcement used for obtaining the metal-metal composites are shown in Table 1. The investigated microcomposite (composite with the addition of Ti microparticles only) was produced by the compocasting process on the apparatus (Figure 1) which consists of a laboratory electric 2 kW resistance furnace (with additional temperature control equipment) and a mixer with a plate-like active part fixed on the mixer shaft.¹⁵ The same process was used for the production of the micro-nanocomposites (composites with the addition of Ti microparticles and Al₂O₃ nanoparticles); only the mechanical alloying pre-processing had been applied beforehand. Designation of the produced metal-metal composites is also shown in Table 1. Reference material was ZA-27 alloy produced by rheocasting (designated as ZA-27 thixo). Rheocasting is a casting process where the semi-solid slurry is generated directly from the liquid and poured into the mould. In the first stage, partial solidification of melt is performed, so the slurry consists of non-dendritic and globular particle. The second stage is the complete solidification in the mould.¹⁶ The applied

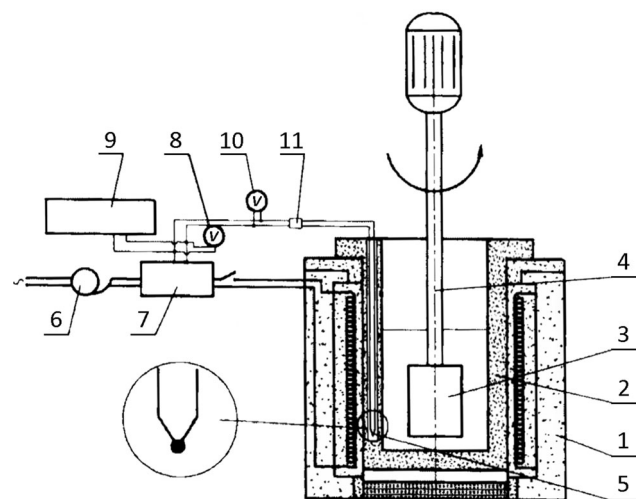


Figure 1. Schematic drawing of the apparatus for compocasting processing (1: resistance furnace, 2: crucible, 3: mixer, 4: mixer shaft, 5: thermocouple, 6–11: devices and instruments for temperature measurement, control and regulation)¹⁵.

technique that has been used to obtain semi-solid slurry with non-dendritic structure was mechanical stirring. At the end of producing process, all samples were hot-pressed (350 °C and 250 MPa) with steel tool, for the purpose of densification. In this way, samples of 30 × 15 × 6 mm were obtained.

During the production of the ZA-27 thixo samples by the rheocasting process, the matrix alloy was first superheated at 550 °C, and the slag was cleaned. After that, the temperature of the melt was reduced at 500 °C, followed by mixing of the melt with a stirrer at 500 rpm, for 5 minutes. Then, with continued mixing, the temperature of the melt was reduced further at 465 °C (cooling rate of 5 °C/min). Additional mixing at this temperature was continued for 8 minutes, after which the melt was poured into a preheated mould (at 480 °C) made of steel.

During the production of the 1Ti samples by the compositing process, the matrix alloy was first superheated at 550 °C, and the slag was cleaned. After that, the temperature of the melt was reduced at 485 °C, followed by mixing of the melt with a stirrer at 500 rpm, for 5 minutes. Then, with continued mixing, the temperature of the melt was reduced further at 465 °C (cooling rate of 5 °C/min). Infiltration of the Ti microparticles, preheated at 100 °C, started at this temperature and lasted for 3 minutes. Additional mixing at this temperature was continued for 10 minutes, after which the melt was poured into a preheated mould (at 480 °C) made of steel.

The 1Ti-0.5Al₂O₃ and 2Ti-0.5Al₂O₃ samples were also produced by the compositing process. The difference is that before the compositing process, mechanical alloying pre-processing (ball milling) was performed. The milling process was carried out in air, at room temperature, with rotational speed of 500 rpm, using 10- and 14-mm-diameter alumina balls (with 60:40 percentage ratio), for 60 minutes. The ZA-27 alloy metal chips-to-nanoparticles weight ratio was 3:1, while the weight ratio alumina ball-to-milling mixture was 5:1. Compositing process started with the matrix alloy superheating at 550 °C, and cleaning of the slag. After that, the temperature of the melt was reduced at 500 °C, followed by mixing of the melt with a stirrer at 250 rpm. Infiltration of the milling mixture (mixture of ZA-27 alloy metal chips and Al₂O₃ nanoparticles), obtained in ball milling process and preheated at 200 °C, started at this temperature and lasted for 3 minutes. After the infiltration, mixing of the melt at increased rate of 500 rpm lasted for 5 minutes. Then, with continued mixing, the temperature of the melt was reduced further at 465 °C (cooling rate of 5 °C/min). Infiltration of the Ti microparticles, preheated at 100 °C, started at this temperature and lasted for 3 minutes. Additional mixing at this temperature was continued for 8 minutes, after which the melt was poured into a preheated mould (at 480 °C) made of steel.

Methods of Characterization

Plate-like samples (15 × 15 × 6 mm) are postulated for microstructural examinations by Tescan Mira 3 FEG scanning electron microscopy (SEM) with electron acceleration voltage of 15 kV. The process of their preparation for testing has the following stages: grinding with the SiC abrasive paper of progressively fine grades (P80, P360 and P600 grit, respectively); polishing with the paste containing Al₂O₃ microparticles (particle size 1–5 µm). Morphology of Ti microparticles and the mixture obtained in ball milling process are also studied by SEM.

The surface microhardness (HV 0.5) was determined on the same plate-like samples that have been used for microstructural examinations. For this purpose, Vickers microhardness tester was used. For each sample, five measurements were taken, in order to exclude possible segregation effects and to obtain average value of the material microhardness which is representative.

Tribological tests were performed in lubricated sliding conditions using a tribometer with block-on-disc configuration (line contact of 6 mm), in accordance with ASTM standard.¹⁷ Blocks were used as wear test samples, i.e. they are made of tested materials, while the disc (counter-body) material was the same for all tests, i.e. quenched and tempered steel EN 42CrMo4 (51–54 HRC). Approximate values of surface roughness (*Ra*) were 0.65 µm (blocks) and 0.17 µm (discs). Lubrication with engine oil (SAE 15W-40, ACEA E3) was enabled by the rotation of the disc immersed into an oil reservoir. Test parameters were: 0.5 m/s (sliding speed), 1000 m (sliding distance) and 100 N (normal load). For each sample, six replicate tests were performed. Wear scar on block was measured after each test, in order to compute the volume loss, while the coefficient of friction was tracked continuously during the test. Worn surfaces of blocks were analysed after testing by SEM.

Results and Discussion

Microstructure

The microstructure of ZA-27 thixo sample is shown in Figure 2. Microconstituents can be clearly distinguished, i.e. dark grey areas of α phase, middle grey areas of $\alpha + \eta$ phase mixture and light grey areas of η phase. The α phase morphology shows transformation of the dendritic structure (which is common for, for example, sand cast ZA-27 alloy) into the non-dendritic structure, i.e. the α phase regions were transformed into a form of irregular ellipse and (in a small amount of) degenerated dendrites. The sand castings of the ZA-27 alloy solidify naturally with coarse dendritic structure, which detrimentally influences plastic properties,^{18,19} as well as its hardness and wear resistance.

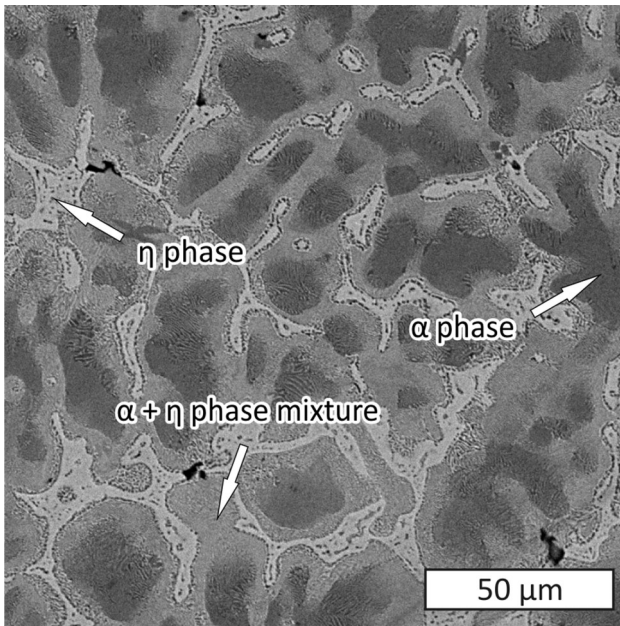


Figure 2. Microstructure of ZA-27 thixo material, SEM.

Transformation of the structure from dendritic to non-dendritic occurred during mixing of the semi-solid melt, due to the influence of shear forces. This is in accordance with the rheological investigations performed by Lehuu et al.²⁰ Interval between liquidus and solidus temperature of the ZA-27 alloy is relatively wide, which is not favourable in casting practice due to problems with the porosity of the castings, but it is very important for the semi-solid processing of ZA-27 alloy.

Morphology of Ti microparticles used in the production of 1Ti microcomposite is shown in Figure 3. According to the

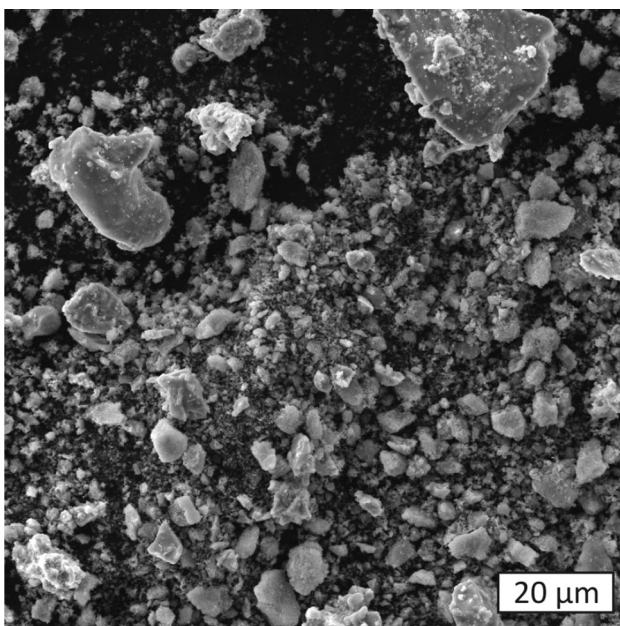


Figure 3. Morphology of Ti microparticles, SEM.

manufacturer data, the average size of the Ti particles is 10 μm, but SEM analysis showed the presence of larger particles too. However, particles larger than 30 μm were not noticed. The SEM analysis also showed that Ti particles have irregular morphology and that in the powder form they are not prone to agglomeration.

The microstructure of 1Ti metal-metal microcomposite is shown in Figure 4. Titanium particles in a produced composite were not well distributed in the ZA-27 alloy matrix, i.e. they were agglomerated (Figure 4a). This is not an unexpected phenomenon considering that the investigations are at the initial stage. In addition, samples were produced by the compocasting process which is cheaper than, for example, powder metallurgy but produce samples of lower quality. Titanium microparticles and their agglomerations can be clearly distinguished as very dark grey areas (denoted in Figure 4a). Imaginary Vickers microhardness indent is also denoted with white lines in Figure 4a, since its size is very important for the analysis of the microhardness values. Larger view of one agglomeration of Ti microparticles is shown in Figure 4b, which is a detail of Figure 4a. Titanium particles size was between 10 and 30 μm, i.e. it corresponded to the size of the initial Ti powder. Figure 4b also shows that Ti particles seem do not touch each other within the agglomeration, i.e. Ti particles boundaries are clearly visible. When this is the case, it is possible to accomplish a better interface between the particles and the matrix, and therefore a better load transfer from the matrix to the particle. This is favourable circumstance which indicates that it is possible to achieve a better distribution and/or to infiltrate higher amount of Ti microparticles in some upcoming experiments.

Morphology of the mixture of ZA-27 alloy metal chips and Al₂O₃ nanoparticles, obtained in ball milling process, which is used in the production of 1Ti-0.5Al₂O₃ and 2Ti-0.5Al₂O₃ micro-nanocomposites, is shown in Figure 5. According to the SEM analysis, it seems that the milling process was successfully performed. The size of the metal chips of the matrix alloy was significantly reduced after 60 min of the milling process.¹³ They became rounded and completely covered with the Al₂O₃ nanoparticles, i.e. “clean” metal chips cannot be noticed. Due to repeated collisions with alumina balls, clusters of nanoparticles in the milling mixture were mostly broken during the milling process. Nevertheless, clusters of Al₂O₃ nanoparticles still can be noticed in the mixture obtained in ball milling process.

The microstructures of 1Ti-0.5Al₂O₃ and 2Ti-0.5Al₂O₃ metal-metal micro-nanocomposites were very similar, so only the microstructure of 1Ti-0.5Al₂O₃ is shown in Figures 6 and 7. The addition of Al₂O₃ nanoparticles induced a significant change in the microstructure. Namely, it can be noticed that the area of the matrix that is filled with particles is larger in relation to the 1Ti metal-metal composite

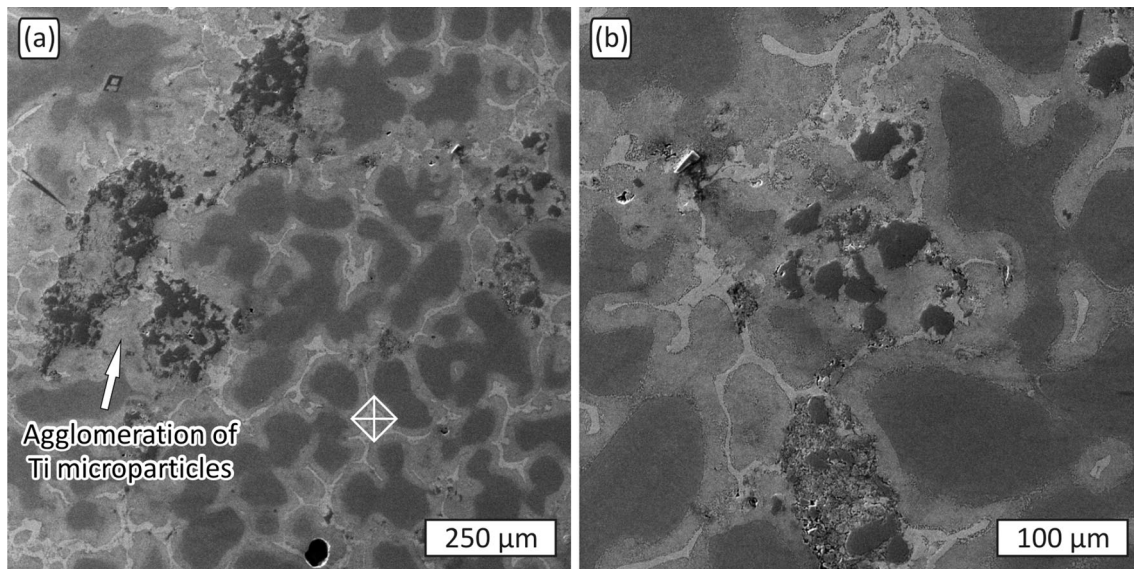


Figure 4. Microstructure of 1Ti metal-metal microcomposite, SEM: (a) general appearance (imaginary Vickers microhardness indent, with average diagonals of 86 μm , is denoted with white lines) and (b) larger view of one agglomeration of Ti microparticles.

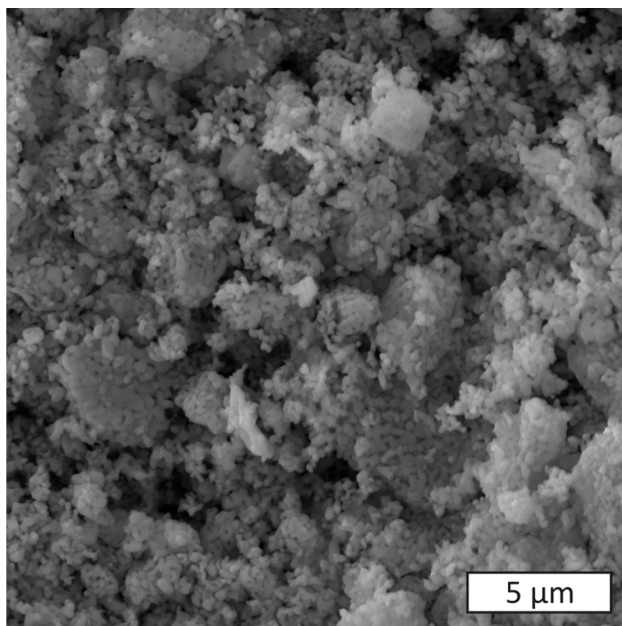


Figure 5. Morphology of mixture of ZA-27 alloy metal chips and Al_2O_3 nanoparticles, obtained in ball milling process, SEM.

(Figure 6a). This is a favourable circumstance that should protect the matrix better during sliding and reduce wear. The Ti particles are clearly visible, while the clusters of the Al_2O_3 nanoparticles are clearly visible only at a higher magnification SEM image, as very bright areas (Figure 6b). The area denoted with rectangle in Figure 6b is presented on separate higher magnification image (Figure 7). It is interesting that clusters of the Al_2O_3 nanoparticles accumulate around the Ti particles, although they were infiltrated separately.

Cracking of large Ti particles was also noticed (Figure 7). This most likely occurred during cooling, due to the high difference in coefficients of linear thermal expansion (CTE) amongst Ti particles and ZA-27 alloy matrix. (CTE for titanium is about 8.6×10^{-6} , and for ZA-27 alloy about 26×10^{-6} .) This means that the bonding between Ti particles and the matrix is good, although the phenomenon itself is not favourable, since it could cause so-called debonding effect and reduce the strength of composite.

Microhardness

The results of the surface microhardness testing are shown in Figure 8. The standard deviation values indicate that the repeatability of the results was below 10%. Nevertheless, this repeatability suggests inhomogeneity of all tested materials, i.e. even of the rheocasted ZA-27 alloy. Prescribed values of hardness for sand/die cast ZA-27 alloy are 113/119 HB.¹⁴ This corresponds to the obtained values of tested materials, which were more or less similar. Only the composite 2Ti-0.5 Al_2O_3 showed more significant increase in hardness (approx. 13%) compared to the rheocasted ZA-27 alloy. Relatively low influence of Ti particles and/or Al_2O_3 nanoparticles can be explained with the fact that the average Vickers microhardness indentation diagonal was approximately 86 μm , which is significantly smaller than the distance between the agglomerations of Ti particles (Figure 4a). On the other hand, by choosing the microhardness values impact of porosity, inclusions and agglomeration of secondary phases on the assessment of matrix hardness is reduced.

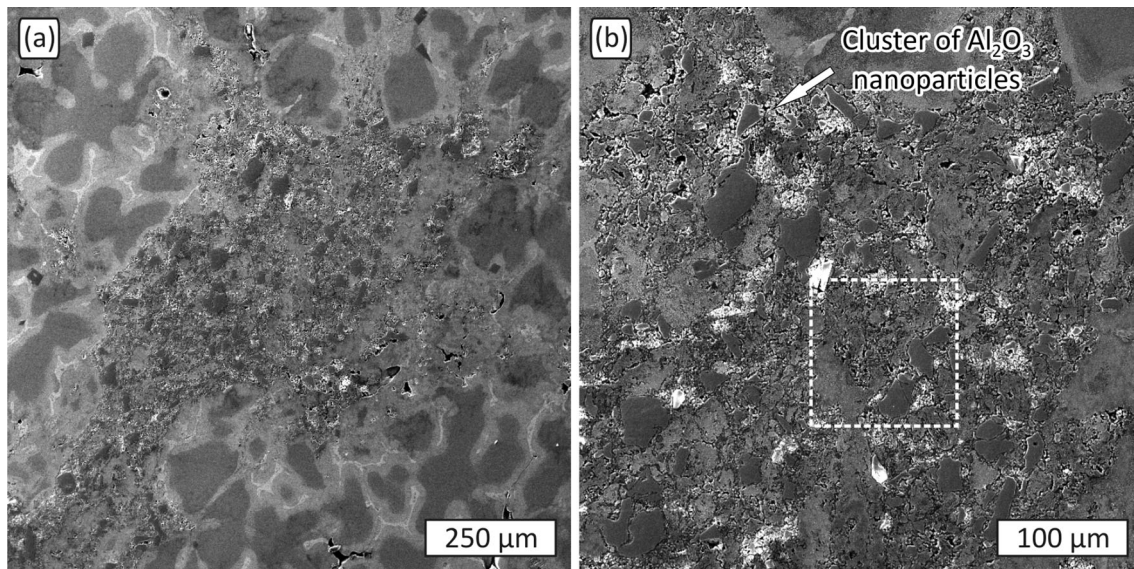


Figure 6. Microstructure of 1Ti-0.5Al₂O₃ metal-metal micro-nanocomposite, SEM: (a) general appearance and (b) distribution of Al₂O₃ nanoparticles clusters (area denoted with rectangle is presented on separate higher magnification image).

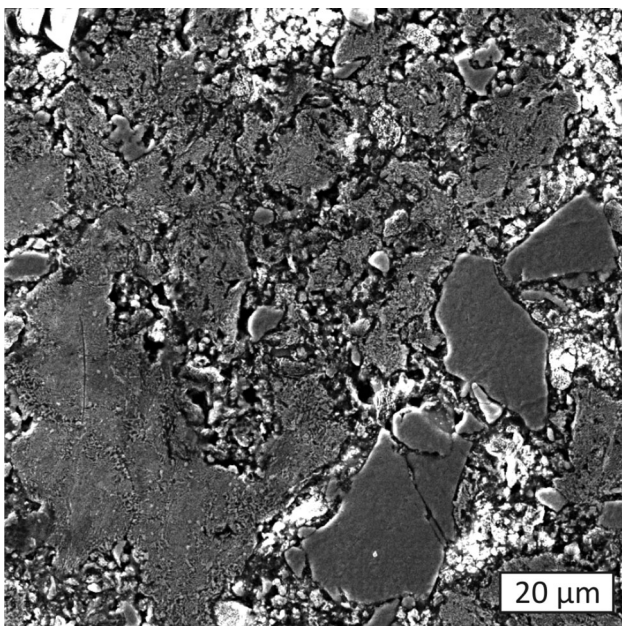


Figure 7. Detail view of the Ti microparticles and Al₂O₃ nanoparticles clusters in the microstructure of 1Ti-0.5Al₂O₃ metal-metal micro-nanocomposite, SEM.

Tribological Properties

The results of tribological testing are presented in Figures 9 and 10. Coefficient of friction (COF) values are calculated for the steady-state period (Figure 9). Their appropriate standard deviations indicate that the repeatability of the results was also below 10%. The interval for the COF values was from 0.04 to 0.06. This means that the sliding most probably was under mixed lubrication conditions. The literature data of COF approximate values for two

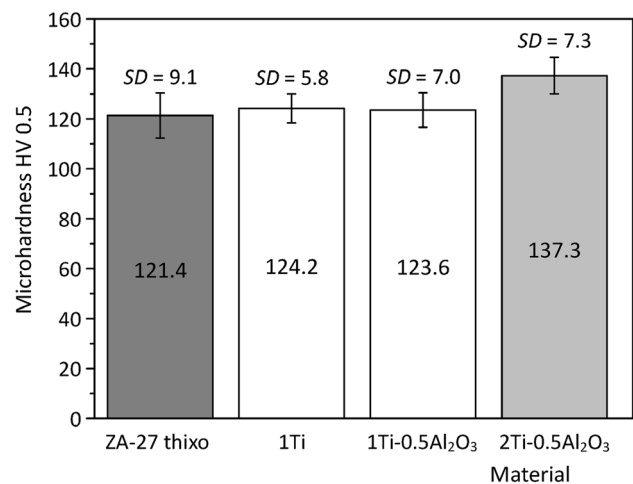


Figure 8. Microhardness values and appropriate standard deviations (SD) of tested materials.

lubrication regimes which bordered mixed lubrication regime are: 0.002–0.05 (elastohydrodynamic lubrication) and 0.05–0.15 (boundary lubrication).^{21,22} The values of COF were in accordance with our previous research conducted under the similar testing conditions.²³ The addition of Ti microparticles and/or Al₂O₃ nanoparticles did not show any significant influence on the COF, i.e. all tested materials showed similar values. This is regular behaviour, since the material influence is relatively low in mixed lubrication regime.²⁴ Higher material influence and noticed inhomogeneity will most probably induce lower repeatability of the COF values, which was not the case.

Wear rate values (in mm³/m) are calculated for the whole testing period, i.e. as total wear rates (Figure 10). This means that the volume loss (in mm³), calculated according

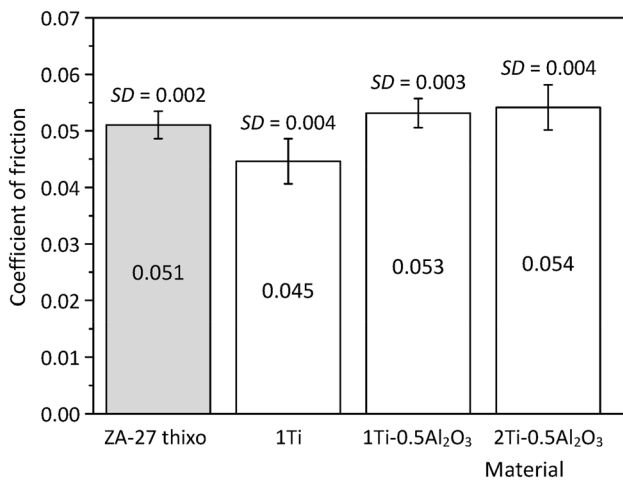


Figure 9. Coefficients of friction of tested materials with their standard deviations (SD).

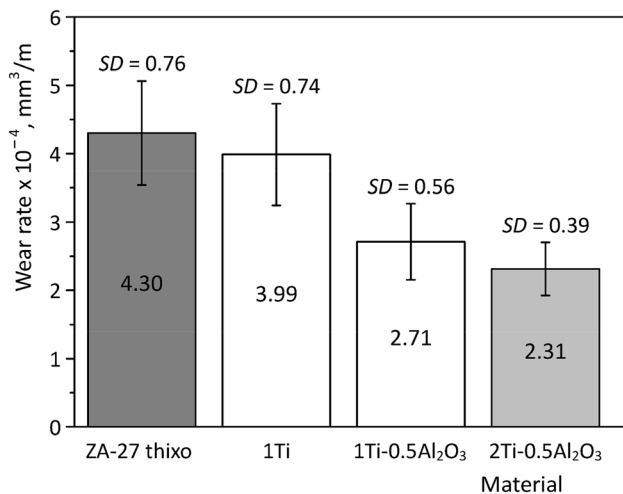


Figure 10. Wear rates of tested materials with their standard deviations (SD).

to ASTM standard,¹⁷ is divided by the total sliding distance of 1000 m. Their appropriate standard deviations were high (up to 20%), and that indicates to relatively low repeatability of the results. This is connected with the observed inhomogeneous structures of tested materials. Structures differ between the samples of the same material, as well as within the sample, which together with other factors results in high dissipation of the results. Any exact correlation between wear rates and microhardness (Figure 8) and/or COF (Figure 9) values of the tested materials could not be established. In spite of the high values of standard deviations and some overlap of the values, mutual relations between the tested materials and trend of wear behaviour are obvious. All wear rate values were of the same order of magnitude (10^{-4} mm³/m), but the wear rate of reference material (ZA-27 thixo) was almost two times higher than the wear rate of micro-nanocomposite with 2 wt% Ti and 0.5 wt% Al₂O₃ (2Ti-0.5Al₂O₃). Obtained wear rate for ZA-27 thixo material (4.30×10^{-4} mm³/m) was very similar to

the wear rate for commercial ZA-27 alloy (4.54×10^{-4} mm³/m), obtained in our previous research conducted under similar testing conditions.²³

The reduction of wear rate of 1Ti microcomposite was only about 7% compared to the reference material (ZA-27 thixo), which suggests that the addition of 1 wt% Ti microparticles did not have major influence on wear rate. This is in accordance with the microstructure of this composite (Figure 4a). The amount of titanium particles was low and they were agglomerated, so they could only partially protect the matrix. Similarly, the reduction of wear rate of 2Ti-0.5Al₂O₃ micro-nanocomposites was about 15% compared to the 1Ti-0.5Al₂O₃ micro-nanocomposite, confirming that the addition of Ti microparticles reduced wear rate, but that the reduction is not too remarkable concerning the high values of standard deviations. The influence of Al₂O₃ nanoparticles addition without the addition of Ti microparticles was not analysed, since the amount of used Al₂O₃ nanoparticles was very low (0.5 wt%); and in our previous study²⁵, we showed that this small amount of nanoparticles reinforcement do not have significant influence on wear resistance either.

On the other hand, the addition of both, Al₂O₃ nanoparticles and Ti microparticles, had higher influence on wear rate. This was reflected in a reduction of wear rate of 1Ti-0.5Al₂O₃ and 2Ti-0.5Al₂O₃ micro-nanocomposites compared to the reference material, which were approximately 37% and 46%, respectively. This reduction is obvious, in spite of the high values of standard deviations, which is of most importance for the application of these materials for manufacturing of the tribological components. The reduction can be explained with better distribution of Ti particles in micro-nanocomposites (Figure 6a) and probably due to some strengthening mechanisms that may be present. The presence of ceramic nanoparticles created fine-grained structure of the matrix alloy (ZA-27), which enhances the mechanical properties of the composite by increasing the dislocation density.¹³ Better distribution of Ti particles practically affected and increased the surface area of the matrix that is filled, and thus protected, with Ti particles. Although the agglomerations of Ti particles were still present in the structure, their negative influence on the wear resistance was reduced since the average wear scar was about 2.7 mm, which was significantly bigger than the distance between the agglomerations of Ti particles.

The SEM analysis of worn surfaces, which were performed after testing, showed that all worn surfaces were very similar. Similar appearance of worn surfaces is in agreement with the wear rates of tested materials (Figure 10), which were of the same order of magnitude. The dominant wear mechanism in all cases was light abrasion, which was more pronounced on materials that shown higher wear rates (Figure 11). Occurrence of adhesive wear was also noticed on worn surfaces of all materials, but only as

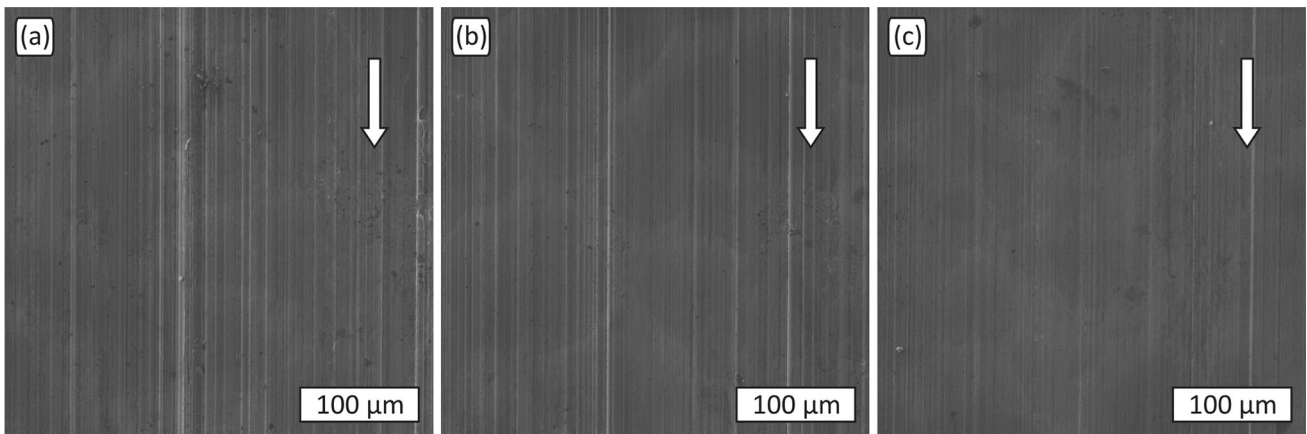


Figure 11. Surfaces of tested materials worn by light abrasion, SEM: (a) ZA-27 thixo material, (b) 1Ti metal-metal microcomposite, and (c) 1Ti-0.5Al₂O₃ metal-metal micro-nanocomposite; arrows represent the sliding direction of counter-body.

isolated and small areas, i.e. only few areas on each worn surface. Some typical appearances are shown in Figure 12. The presence of abrasive wear was more or less regular, since it is the most common type of wear. On the other hand, testing was in poorly lubricated sliding contacts under relatively high load (line contact), which are the precondition for occurrence of adhesive wear. Noticed wear mechanisms also corresponded to the wear factor values, which were very easy to calculate, i.e. wear rate values were divided by normal load, which was 100 N. Calculated wear factors for ZA-27 thixo material ($4.30 \times 10^{-6} \text{ mm}^3/\text{Nm}$), 1Ti microcomposite ($3.99 \times 10^{-6} \text{ mm}^3/\text{Nm}$), 1Ti-0.5Al₂O₃ micro-nanocomposite ($2.71 \times 10^{-6} \text{ mm}^3/\text{Nm}$) and 2Ti-0.5Al₂O₃ micro-nanocomposite ($2.31 \times 10^{-6} \text{ mm}^3/\text{Nm}$) were also of the same order of magnitude ($10^{-6} \text{ mm}^3/\text{Nm}$). The literature data of wear factor values for metallic materials in sliding contact are: 10^{-9} – $10^{-6} \text{ mm}^3/\text{Nm}$ (boundary lubrication) and 10^{-7} – $10^{-2} \text{ mm}^3/\text{Nm}$ (unlubricated and adhesive wear).²⁶ Although it commonly occurs, the transfer of

material from the counter-body was not noticed during the SEM analysis of the worn surfaces of tested materials.

Conclusions

The metal-metal composites with Zn-Al alloy base and addition of Ti microparticles and alumina nanoparticles can be produced by the applied compositing process. It is necessary to additionally improve the process, primarily in the domain of better distribution of micro- and nanoparticles in the metal matrix. The most influential feature of the microstructure of investigated metal-metal composites was the distribution of Ti particles, which make agglomerations. This distribution was improved with the addition of Al₂O₃ nanoparticles.

Microhardness was similar for all tested materials, as well as coefficient of friction values. Relatively low influence of Ti microparticles and/or Al₂O₃ nanoparticles on matrix microhardness is due to the fact that the microhardness

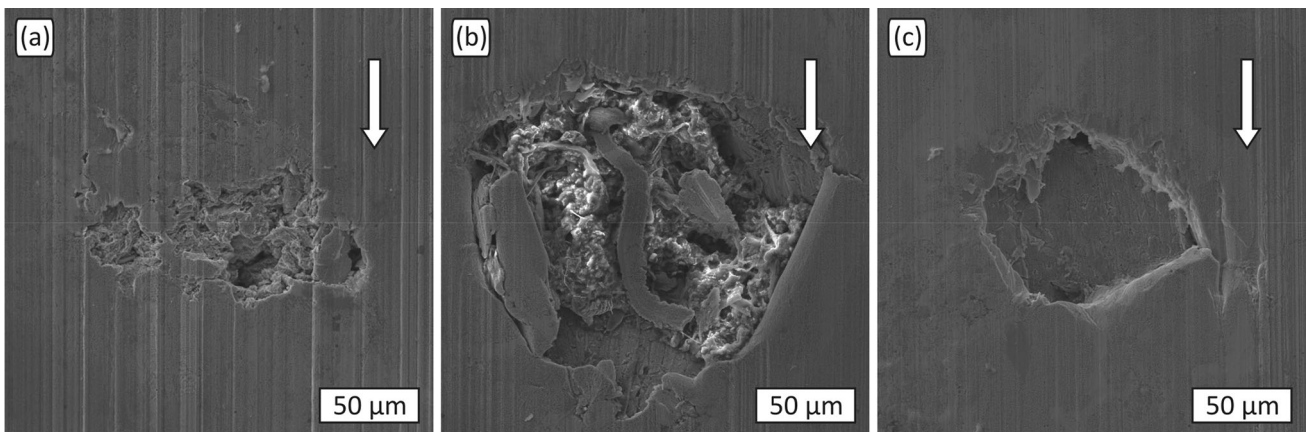


Figure 12. Presence of adhesive wear on worn surfaces of tested materials, SEM: (a) ZA-27 thixo material, (b) 1Ti metal-metal microcomposite, and (c) 1Ti-0.5Al₂O₃ metal-metal micro-nanocomposite; arrows represent the sliding direction of counter-body.

indentation diagonal was significantly smaller than the distance between the agglomerations of Ti and Al₂O₃ particles. On the other hand, since mixed lubrication regime was obtained during the testing, the material influence on friction was very little pronounced.

Wear values were in correlation with the microstructures, i.e. composites with better distribution of Ti particles showed higher wear resistance. Micro-nanocomposites (composites with the addition of Ti microparticles and Al₂O₃ nanoparticles) showed noticeable decrease of wear over the reference material (ZA-27 alloy produced by rheocasting) due to the synergetic effect Ti microparticles and Al₂O₃ nanoparticles, i.e. better distribution of Ti microparticles and probably due to the possible strengthening mechanisms induced by Al₂O₃ nanoparticles.

Acknowledgements

This work has been performed as a part of activities within the project 451-03-68/2020-14/200105, supported by the Republic of Serbia, Ministry of Education, Science and Technological Development, and its financial help is gratefully acknowledged. Marcela Pokusová acknowledges the project APVV-16-0485, supported by the Slovak Research and Development Agency. Mara Kandeveva acknowledges the project LH 07/28-15.12.2016, funded by the National Science Fund at the Ministry of Education and Science, Bulgaria. Collaboration through the CEEPUS network CIII-BG-0703 and the bilateral project No. 451-03-478/2018-09/02 between Republic of Serbia and People's Republic of China is also acknowledged.

REFERENCES

1. E. Gervais, R.J. Barnhurst, C.A. Loong, An analysis of selected properties of ZA alloys. *J Metals (JOM)* **37**(11), 43–47 (1985)
2. E.J. Kubel Jr., Expanding horizons for ZA alloys. *Adv. Mater. Processes* **132**(1), 51–57 (1987)
3. A. Rac, M. Babić, R. Ninković, Theory and practice of Zn-Al sliding bearings. *J Balkan Tribol Assoc* **7**(3–4), 234–240 (2001)
4. D. Yousefi, R. Taghiabadi, M.H. Shaeri, P. Abedinzadeh, Enhancing the mechanical properties of Si particle reinforced ZA22 composite by Ti-B modification. *Int J Metalcast* (2020). <https://doi.org/10.1007/s40962-020-00447-w>
5. F. Vučetić, S. Veličković, A. Milivojević, A. Vencl, A review on tribological properties of microcomposites with ZA-27 alloy matrix. In: 15th International Conference on Tribology – SERBIATRIB '17, Kragujevac (Serbia), 17-19.05.2017, Proceedings, pp. 169-176

6. M.K. Gopi, K.K. Praveen, M.S. Naga, J.R. Babu, N.R.M.R. Bhargava, Metal-metal composites—An innovative way for multiple strengthening. *Mater Today: Proc* **4**(8), 8085–8095 (2017)
7. Z.R. Yang, S.Q. Wang, M.J. Gao, Y.T. Zhao, K.M. Chen, X.H. Cui, A new-developed magnesium matrix composite by reactive sintering. *Compos. A Appl. Sci. Manuf.* **39**(9), 1427–1432 (2008)
8. S.T. Kumar, M. Gupta, Improving mechanical performance of Al by using Ti as reinforcement. *Compos Part A: Appl Sci Manuf* **38**(3), 1010–1018 (2007)
9. E.T. Basiri, H.R.H. Madaah, S.M.R. Seyed, On the fracture toughness behavior of in-situ Al-Ti composites produced via mechanical alloying and hot extrusion. *J Alloys Compounds* **681**, 12–21 (2016)
10. S.F. Hassan, M. Gupta, Development of ductile magnesium composite materials using titanium as reinforcement. *J. Alloy. Compd.* **345**(1–2), 246–251 (2002)
11. P. Pérez, G. Garcés, P. Adeva, Mechanical properties of a Mg–10(vol %)Ti composite. *Compos Sci Technol* **64**(1), 145–151 (2004)
12. K.N. Braszczyńska-Malik, E. Przełoczyńska, Analyses of AM50-Ti_p metal-metal composite microstructure. *J. Alloy. Compd.* **731**, 1181–1187 (2018)
13. B. Bobić, A. Vencl, J. Ružić, I. Bobić, Z. Damnjanović, Microstructural and basic mechanical characteristics of ZA27 alloy-based nanocomposites synthesized by mechanical milling and compocasting. *J. Compos. Mater.* **53**(15), 2033–2046 (2019)
14. ASTM B 86, Standard specification for zinc and zinc-aluminum (ZA) alloy foundry and die castings
15. A. Vencl, I. Bobić, M.T. Jovanović, M. Babić, S. Mitrović, Microstructural and tribological properties of A356 Al-Si alloy reinforced with Al₂O₃ particles. *Tribol. Lett.* **32**(3), 159–170 (2008)
16. M.M. Shehata, S. El-Hadad, M.E. Moussa, M. El-Shennawy, Optimizing the pouring temperature for semisolid casting of a hypereutectic Al-Si alloy using the cooling slope plate method. *Int J Metalcast* (2020). <https://doi.org/10.1007/s40962-020-00465-8>
17. ASTM G 77, Standard test method for ranking resistance of materials to sliding wear using block-on-ring wear test
18. W.K. Krajewski, Structure and properties of high-aluminium zinc alloys inoculated with Ti addition. *Archives of Foundry* **5**(15), 231–240 (2005)
19. P.K. Krajewski, A.L. Greer, W.K. Krajewski, Main directions of recent works on Al-Zn-based alloys for foundry engineering. *J. Mater. Eng. Perform.* **28**(7), 3986–3993 (2019)
20. H. Lehuy, J. Masounave, J. Blain, Rheological behaviour and microstructure of stir-casting zinc-aluminium alloys. *J. Mater. Sci.* **20**(1), 105–113 (1985)

21. B.J. Hamrock, S.R. Schmid, B.O. Jacobson, *Fundamental of Fluid Film Lubrication* (Marcel Dekker Inc, New York, 2004).
22. A. Rac, Basics of Tribology, Faculty of Mechanical Engineering, University of Belgrade, Belgrade, 1991, pp. 7-23 (in Serbian)
23. A. Vencel, I. Bobić, F. Vučetić, B. Bobić, J. Ružić, Structural, mechanical and tribological characterization of Zn25Al alloys with Si and Sr addition. *Mater. Des.* **64**, 381–392 (2014)
24. M.B. Dobrica, M. Fillon, Mixed lubrication, in *Encyclopedia of tribology*. ed. by Q.J. Wang, Y.-W. Chung (Springer, New York, 2013), pp. 2284–2291
25. A. Vencel, I. Bobić, B. Bobić, K. Jakimovska, P. Svoboda, M. Kandevo, Erosive wear properties of ZA-27 alloy-based nanocomposites: Influence of type, amount and size of nanoparticle reinforcements. *Friction* **7**(4), 340–350 (2019)
26. K. Kato, K. Adachi, Wear mechanisms, in *Modern tribology handbook*. ed. by B. Bhushan (CRC Press, Boca Raton, 2001)

Publisher's Note Springer Nature remains neutral with regard to jurisdictional claims in published maps and institutional affiliations.